Acta Crystallographica Section D
Biological Crystallography
ISSN 0907-4449

Human glutamate carboxypeptidase II inhibition: structures of GCPII in complex with two potent inhibitors, quisqualate and 2-PMPA

Jeroen R. Mesters,* Karen Henning and Rolf Hilgenfeld

Institute of Biochemistry, Center for Structural and Cell Biology In Medicine, University of Lübeck, Ratzeburger Allee 160, Lübeck 23538, Germany

Correspondence e-mail: mesters@biochem.uni-luebeck.de

Received 10 February 2007
Accepted 23 February 2007

PDB References: GCPII–quisqualic acid complex, 2jbk, r2jbksf; GCPII–2-PMPA complex, 2jbj, r2jbjsf.

Human glutamate carboxypeptidase II (GCPII) occurs in the central nervous system as well as in human prostate (where it is called prostate-specific membrane antigen; PSMA). Inhibitors of the enzyme have been shown to provide neuroprotection, but may also be useful for the detection, imaging and treatment of prostate cancer. Crystal structures were determined of the extracellular part of GCPII (amino-acid residues 44–750) in complex with two potent inhibitors, quisqualate and 2-PMPA (the strongest GCPII inhibitor to date), at resolutions of 3.0 and 2.2 Å, respectively. In addition, models were constructed for binding of the inhibitors willardiine, homoibotenate, L-2-amino-4-phosphonobutanoic acid and L-serine-*O*-sulfate to the S1′ site of the enzyme. The common denominator for high-affinity binding to the S1′ site is the formation of two strong salt bridges.

1. Introduction

More than 20 years ago, Koller and Coyle demonstrated that the hydrolysis of the endogenous neuropeptide *N*-acetyl-L-aspartyl-L-glutamic acid (NAAG) by the then unidentified N-acetylated α-linked acidic dipeptidase (NAALADase; Robinson *et al.*, 1987) could be specifically inhibited by serine-*O*-sulfate, quisqualate, ibotenate and glutamate with apparent K_i values in the nanomolar range (Koller & Coyle, 1985). The prostate-tumour marker PSMA (prostate-specific membrane antigen; PDB code 1z8l; Davis *et al.*, 2005), a folate polyglutamate hydrolase that is overexpressed in cancer tissue, is identical to NAALADase and both enzymes are today known by the name glutamate carboxypeptidase II (GCPII; EC 3.4.17.21; peptidase subfamily M28B; MEROPS clan MH; Rawlings *et al.*, 2004). Human GCPII is a heavily N-glycosylated, membrane-anchored, dinuclear zinc metalloenzyme of 750 amino-acid residues that has been shown to catalyze the hydrolysis of the synaptic neurotransmitter NAAG to yield *N*-acetyl-L-aspartate and L-glutamate and the hydrolysis of folylpoly-γ-L-glutamate, ultimately releasing folate. In addition to the two zinc ions in the active site, a chloride and a calcium ion were located in the crystal structure of GCPII (Mesters *et al.*, 2006) and both ions are required for the hydrolytic activity of the enzyme (Koller & Coyle, 1985; Robinson *et al.*, 1987). Whereas the binding of Ca^{2+} appears to be essential for formation of the GCPII homodimer (the biologically active form of the enzyme; Troyer *et al.*, 1995; Schulke *et al.*, 2003), the Cl^- ion is located in the S1 pocket,

where it apparently plays an important role in substrate binding. Phosphate, sulfate, dithiothreitol and metal chelators (EGTA, EDTA and *o*-phenanthroline) inhibit NAAG hydrolysis, while cobalt and other metal ions substituting for Zn^{2+} may stimulate NAAG catabolism (Robinson *et al.*, 1987; Stauch *et al.*, 1989).

Of the various products released by GCPII, glutamate is a neurotransmitter that is excitotoxic at elevated levels and folate is a cofactor for numerous enzymes involved in nucleotide biosynthesis (*e.g.* in proliferating tissue). As a consequence, inhibitors of GCPII have been found on the one hand to provide neuroprotection (Slusher *et al.*, 1999) and on the other hand have been patented for the possible detection, imaging and treatment of prostate cancer (US Patent 6 875 886). In contrast to the less specific S1 pocket of the enzyme (which can accommodate aspartate or glutamate), the S1′ pocket has a clear preference for glutamic acid residues (K_i = 0.46 µ*M*; Koller & Coyle, 1985) and it is therefore not surprising that several glutamate analogues are efficient inhibitors of GCPII. Notably, the X-ray structure of GCPII (Mesters *et al.*, 2006) revealed an induced-fit mechanism. Its 'glutarate sensor' (a β-hairpin encompassing residues Lys699 and Tyr700) probes the P1′ position of the substrate for the presence of two carboxyl moieties, thereby strongly selecting for glutarate-like compounds. α-Amino-3,5-dioxo-1,2,4-oxadiazolidine-2-propanoic acid (quisqualic acid or quisqualate; K_i = 0.4 µ*M*; Koller & Coyle, 1985) is a glutamate analogue obtained from the seeds and fruits of *Quisqualis indica* (rangoon creeper) or *Q. chinensis* (red jasmine). The X-ray structure of quisqualic acid was solved in the mid-1970s to a resolution of 0.58 Å (Flippen & Gilardi, 1976). Besides quisqualate, willardiine [β-(2,4-dihydroxypyrimidin-1-yl)-alanine, a uracilylalanine found in plants] and homoibotenate [HIBO, 2-amino-3-(3-hydroxyisoxazol-5-yl)propionic acid] are prime examples of glutamate mimetics (Fig. 1). The parent compound of HIBO, ibotenic acid, a toxic psychoactive compound from *Amanita muscaria* (fly agaric or magic mushroom), preferentially activates aspartate receptors. Elongation of the side chain of ibotenic acid by one C atom yields homoibotenic acid, which turns this compound into a glutamate-receptor agonist like quisqualate. L-Serine-*O*-sulfate (L-SOS; K_i = 0.1 µ*M*; Koller & Coyle, 1985) and L-2-amino-4-phosphonobutanoic acid (L-AP4, with a phosphate moiety replacing the glutamate γ-carboxyl group; K_i = 3.9 µ*M*; Koller & Coyle, 1985) are two more examples of bona fide glutamate homologues. Furthermore, 2-phosphonomethyl pentanedioic acid (2-PMPA, the most potent GCPII inhibitor to date) was demonstrated to efficiently block GCPII activity (K_i = 0.2 n*M*; Jackson *et al.*, 1996) and to reduce ischaemic brain injury (Slusher *et al.*, 1999).

Here, we report two crystal structures of the extracellular part of fully glycosylated human GCPII (amino-acid residues 44–750) in complex with the potent inhibitors quisqualic acid (data collected at 263 K) and 2-PMPA (data collected at 100 K) at 3.0 and 2.2 Å resolution, respectively. The latter is the first cryo-crystallographic structure of GCPII reported at a resolution better than 3.5 Å; to date, it has proven very difficult to flash-cool crystals of this enzyme (Mesters *et al.*, 2006; Davis *et al.*, 2005). In addition to these X-ray structures, we constructed models of GCPII complexes with willardiine, HIBO, L-AP4 and L-SOS. The structural information obtained in this study allows a detailed analysis of the requirements for high-affinity binding to the S1′ site of human GCPII.

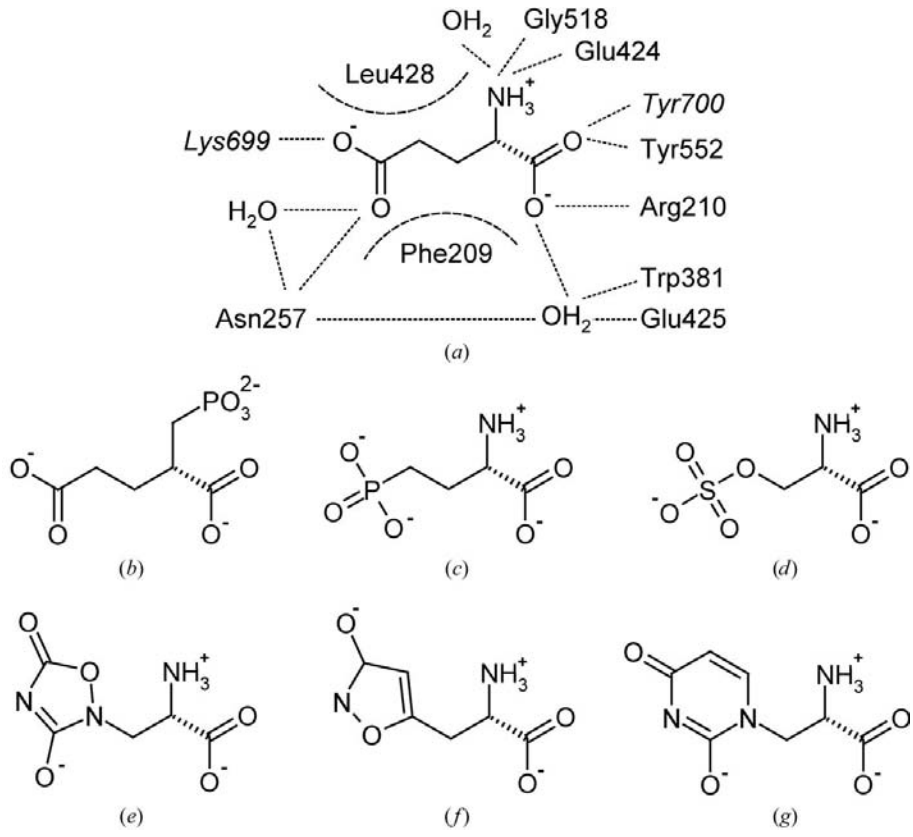

Figure 1
(*a*) Binding mode of glutamate to the S1′ pocket of GCPII. (*b*)–(*g*) Chemical formulae of 2-PMPA (*b*), L-AP4 (*c*), L-SOS (*d*), quisqualate (*e*), HIBO (*f*) and willardiine (*g*).

2. Materials and methods

2.1. Crystallization and structure determination

The cloning, expression and purification of recombinant human GCPII have been described previously (Barinka *et al.*, 2002). Small aliquots of the concentrated protein (*i.e.* 10 mg ml^{-1} in 20 m*M* Tris–HCl, 100 m*M* NaCl pH 8.0) were stored at 193 K. L-Quisqualic acid (the active enantiomer) was obtained from Fluka. A stock solution was

prepared by dissolving 1 mg of the inhibitor in 66 µl 0.1 *M* NaOH (final concentration of 80 m*M*). (*R*,*S*)-2-phosphonomethyl pentanedioic acid, 2-PMPA, a racemic mixture (Jackson *et al.*, 1996), was provided by Guilford Pharmaceuticals Inc. (Baltimore, MD, USA) and the inhibitor was dissolved in distilled water to a final concentration of 50 m*M*. The protein stock solution was mixed with a 1/10 volume of the individual inhibitor solution and crystallization droplets were set up by combining 2 µl GCPII–inhibitor mixture and 2 µl reservoir solution containing 15%(*w*/*v*) PEG 1500, 5%(*v*/*v*) PEG 400, 100 m*M* HEPES, 100 m*M* NaCl pH 7.4. Crystals were grown by the hanging-drop vapour-diffusion method at room temperature. Only very small crystals could be obtained for the quisqualate complex, explaining the lower resolution of this structure.

Diffraction data from single crystals were either collected at 263 K using synchrotron radiation on EMBL beamline X11 (wavelength 0.812 Å) at the Deutsches Elektronen Synchrotron (DESY) or at 100 K using synchrotron radiation on beamline ID29 (wavelength 1.283 Å) at the European Synchrotron Radiation Facility (ESRF). Both beamlines were equipped with a MAR CCD detector (X-ray Research, Hamburg) and the data sets collected were processed using the *HKL* package (HKL Research Inc., Charlottesville, USA). To date, it has been very difficult to cryocool crystals of GCPII (Mesters *et al.*, 2006) or PMSA (Davis *et al.*, 2005). The 2-PMPA complex crystal used in this study was a rare exception, which we were unable to repeat for the quisqualate complex.

Since the crystals were isomorphous to those described previously (Mesters *et al.*, 2006), the structures were determined by difference Fourier methods. The structural model of the GCPII polypeptide as elucidated in complex with GPI-18431 (PDB code 2c6c; Mesters *et al.*, 2006) was used as an initial template for model building of the current complexes. Model refinement and reconstruction were carried out using *REFMAC*5 (Murshudov *et al.*, 1997; Collaborative Computational Project, Number 4, 1994) and *Coot* (Emsley & Cowtan, 2004), respectively. Because of the low resolution, only an overall temperature factor was refined for the quisqualate complex. Also, while an initial $R_{\rm free}$ was calculated for this structural model, all reflections were used in the refinement. The final statistics of the structural refinements and the basic characteristics of the models are presented in Table 1.

Table 1
Refinement statistics and model quality.

Complex	2-PMPA	Quisqualate
No. of crystals	1	1
Temperature (K)	100	263
Space group	*I*222	*I*222
Unit-cell parameters (Å)	*a* = 100.76, *b* = 130.98, *c* = 159.61	*a* = 103.14, *b* = 130.76, *c* = 159.99
Resolution range (Å)	35–2.20 (2.28–2.20)	50–3.0 (3.11–3.00)
No. of unique reflections	52532	20663
Overall completeness (%)	95.9 (81.2)	93.2 (94.2)
$R_{\rm sym}$†	0.09 (0.48)	0.15 (0.64)
$I/\sigma(I)$	14.3 (3.1)	9.7 (2.5)
Redundancy	5.2	5.0
No. of atoms refined		
Protein + carbohydrate	5318	5318
Inhibitor	14	13
Zn^{2+}, Ca^{2+}, Cl^{-}	4	4
Waters	402	19
Refinement		
Test-set size (%)	2.6	5.0
$R_{\rm cryst}$‡	0.192	0.210 (including test set)
$R_{\rm free}$	0.238	0.277 (initial)
$F_{\rm o}$, $F_{\rm c}$ correlation coefficient	0.953	0.912
Mean *B* value (Å^2)	43.06	35.0 (overall)
Wilson plot *B* (Å^2)	37.26	48.76
R.m.s. deviations		
Bond lengths (Å)	0.023	0.024
Bond angles (°)	2.077	2.312
Ramachandran plot, disallowed	2 residues	3 residues

† $R_{\rm sym} = \sum_{hkl}\sum_{i=1}^{N}|\langle I^{hkl}\rangle - I_i^{hkl}|/\sum_{hkl}\sum_{i=1}^{N} I_i^{hkl}$. ‡ $R_{\rm cryst} = \sum_{hkl}||F_{\rm obs}| - k|F_{\rm calc}||/\sum_{hkl}|F_{\rm obs}|$.

2.2. Modelling of GCPII complexes with other glutamate analogues

Because of their very strong resemblance to quisqualic acid (see Fig. 1), we separately modelled willardiine and homoibotenate (HIBO) on the basis of the refined 3.0 Å GCPII–quisqualate structure using *SYBYL* (v.7.2.5, Tripos Inc., St Louis, USA). Similarly, L-AP4 (L-2-amino-4-phophonobutanoic acid) and L-SOS (L-serine-*O*-sulfate) were separately modelled on the basis of the refined 2.2 Å GCPII–2-PMPA structure. For an overall comparison of the binding of the different inhibitors to the S1′ site of GCPII, all structures and models were superpositioned using the program *ALIGN* (Cohen, 1997). Figures were prepared using the *PyMOL* molecular graphics suite (DeLano Scientific LLC, South San Francisco, USA).

3. Results

3.1. Overall structure and active site of GCPII

We have previously described the 2.0 Å structure of human glutamate carboxypeptidase II (GCPII; amino-acid residues 44–750) in detail (Mesters *et al.*, 2006; see also Davis *et al.*, 2005). Briefly, the extracellular part of recombinant GCPII folds into three distinct domains (Fig. 2*a*), all of which are directly involved in substrate binding: the protease domain (domain I, residues 57–116 and 352–590), the apical domain (domain II, residues 117–351) and the C-terminal domain (residues 591–750). Crystals of the complexes of GCPII with quisqualate or 2-PMPA were fully isomorphous to the crystalline complex of the enzyme with GPI-18431 (PDB code 2c6c; Mesters *et al.*, 2006). In both structures presented here, two zinc ions in the active site, a chloride ion in the S1 pocket (coordinated to the side chain of Arg534), a calcium ion close to the dimer interface and seven (out of ten) N-linked carbohydrate chains were clearly visible in the electron-density maps. Glu424 is the likely acid/base of GCPII (Speno *et al.*, 1999). Zn(1) is coordinated to His377, Asp387 and Asp453, and Zn(2) is coordinated to Asp387, Glu425 and

His553. In the complex with quisqualate, which does not chelate the zinc ions, the metal centres are bridged by a bidentate water (or hydroxyl) ligand and the distance between them is 3.3 Å. In contrast, the phosphonate moiety of 2-PMPA replaces the bridging water (or hydroxyl) and the distance between the zinc ions increases to 3.63 Å. This confirms our earlier observation that the Zn···Zn distance is shorter when the metal ions are not ligated by an inhibitor (Mesters *et al.*, 2006). The overall r.m.s. deviations of the C^{α} atoms between the GPI-18431 complex structure (Mesters *et al.*, 2006) on the one hand and the quisqualate and 2-PMPA complexes on the other are 0.31 Å for 667 C^{α} pairs (out of 682 compared) and 0.30 Å for 676 C^{α} pairs (out of 682), respectively. These values are close to the experimental error.

3.2. 2-PMPA and quisqualate binding to the S1′ pocket of GCPII

Seven amino-acid residues basically make up the S1′ pocket: Gly427, Gly518 and the side chains of Phe209, Asn257, Leu428, Lys699 and Tyr700 (Fig. 1*a*). The latter two residues belong to the so-called glutarate sensor that probes the identity of the P1′ residue *via* an induced-fit mechanism (Mesters *et al.*, 2006). In the free enzyme, the loop carrying Lys699-Arg700 is withdrawn from the S1′ site. Residues of all three domains are involved in inhibitor and presumably substrate binding. The dimensions of the S1′ pocket are roughly 8.3 Å (Phe209 C^{ζ}···Gly427 C) by 8.3 Å (Asn257 $N^{\delta2}$··· Gly518 C^{α}) by 8.4 Å (quisqualate C^{α}···Lys699 N^{ζ}).

A close inspection of the electron-density maps revealed that only the (2*S*)-stereoisomer of 2-phosphonomethyl pentanedioic acid (2-PMPA) was bound to GCPII, even though the crystals were grown in the presence of the racemate (see also Tsukamoto *et al.*, 2005). The glutarate portion of 2-PMPA occupies the S1′ site (Fig. 2*b*), while its phosphono moiety coordinates the active-site zinc ions. The binding mode of 2-phosphonomethyl pentanedioic acid is comparable to that observed for GPI-18431, the iodobenzyl derivative of 2-PMPA. One carboxylic group interacts with the hydroxyl groups of Tyr552 (2.98 Å) and Tyr700 (at 2.40 Å), the guanidinium moiety of Arg210 (salt bridge, $N^{\eta1}$ at 2.66 Å) and a water molecule (2.55 Å). This water is in turn hydrogen bonded to Trp381 $N^{\varepsilon1}$ (at 2.94 Å) and the main-chain carbonyl (at 2.73 Å) and $O^{\varepsilon1}$ (at 2.87 Å) of Glu425. The other carboxylic group accepts a hydrogen bond from Asn257 $N^{\delta2}$ (2.85 Å) and a water molecule (at 2.63 Å, which is in turn in contact with Asn257 $O^{\delta2}$) and forms a strong salt bridge with Lys699 N^{ζ} (hydrogen bond, 2.71 Å). Two of the O atoms of the phosphono moiety coordinate to the active-site zinc ions: one O atom is positioned in between the two zinc ions with distances of 2.00 and 2.61 Å, thereby replacing the active-site water/hydroxyl, while the other O atom coordinates Zn(2) only, at a distance of 2.08 Å, and further accepts a hydrogen bond from Tyr552 OH (2.48 Å). The orientation of the phosphono moiety deviates only slightly from that observed for bound GPI-18431 (Mesters *et al.*, 2006).

The two faces of the 3,5-dioxo-1,2,4-oxadiazolidine moiety of quisqualic acid are approached by Leu428 from one side and Phe209 from the other (Figs. 2*c* and 3). The exocyclic oxygen at position 5 accepts a hydrogen bond from Asn257 $N^{\delta2}$ (2.0 Å), while that at position 3 is hydrogen bonded to the ε-amino group of Lys699 (3.2 Å) and the main-chain amide of Gly518 (3.1 Å). The heterocyclic moiety of quisqualic acid is negatively charged and thus also forms a strong ionic interaction with the ε-amino group of Lys699. Hence, the oxadiazolidine ring of quisqualic acid occupies the S1′ pocket in a fashion akin to the γ-carboxylate group of glutamic acid. Similar to glutamate and 2-PMPA, the α-carboxylate group is engaged in a salt bridge with the guanidinium moiety of Arg210 ($N^{\eta1}$ at 2.6 Å) and makes hydrogen bonds with the hydroxyl groups of Tyr552 (3.4 Å), Tyr700 (at 2.4 Å) and a water molecule (at 2.9 Å), which in turn is hydrogen bonded to Trp381 and Glu425. The α-amino group of quisqualic acid donates hydrogen bonds to a water

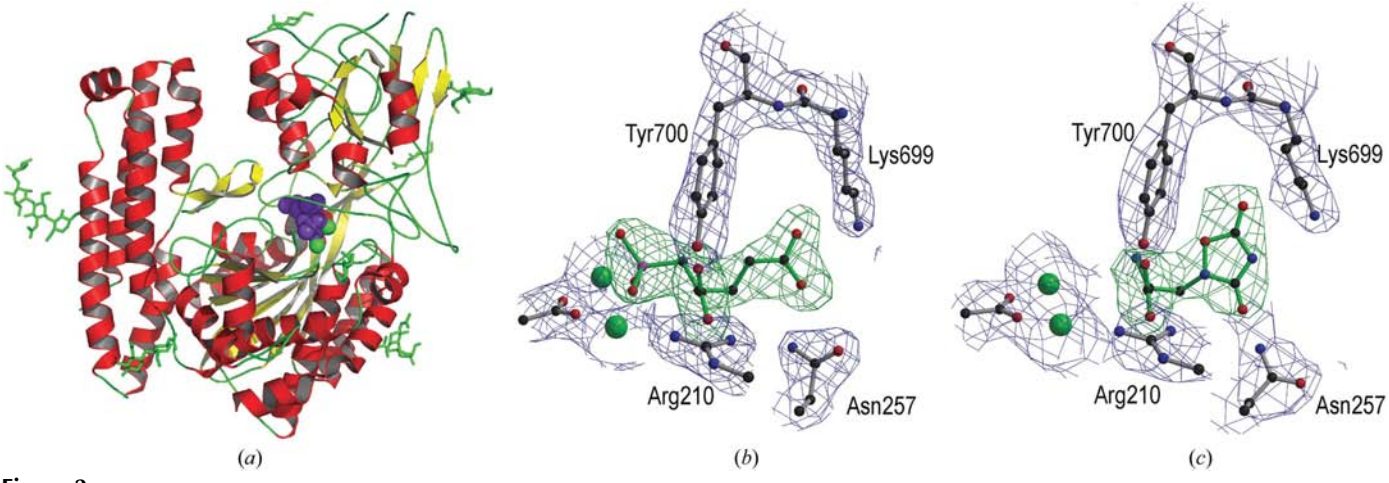

Figure 2
(*a*) Overall structure of GCPII. Zinc ions, green; 2-PMPA (space-filling), purple. (*b*) and (*c*) $2|F_o| - |F_c|$ electron density (blue, contoured at 1σ above the mean) for the 2-PMPA (*b*) and quisqualate (*c*) complexes. The ligand-OMIT $|F_o| - |F_c|$ difference maps, contoured at 3σ above the mean, are superimposed in green. Zinc ions are shown as green spheres.

molecule, to Glu424 $O^{\varepsilon 2}$ and to the main-chain carbonyl of Gly518.

3.3. Modelling of analogues into the S1′ pocket of GCPII and overall analysis

The S1′ pocket of GCPII has a reasonable affinity for glutamic acid ($IC_{50} \simeq 30\ \mu M$; Robinson *et al.*, 1987) and it is therefore not surprising that glutamate mimetics are inhibitors of GCPII. On the basis of the two X-ray structures, we constructed models for S1′-bound willardiine, homoibotenate (HIBO), L-2-amino-4-phophonobutanoic acid (L-AP4) and L-serine-*O*-sulfate (L-SOS). A superimposition of all the inhibitors is presented in Fig. 3. The side chain of Asn257 is seen to adopt different orientations depending on the size of the bound substrate (compare the quisqualate and 2-PMPA structures in Figs. 2*b* and 2*c*). Also, the side chain of Lys699 will have to move out of the way slightly in order to accommodate the slightly larger pyrimidine ring of willardiine. Visual inspection of the S1′ pockets confirms that both Asn257 and Lys699 indeed have sufficient breathing space available to accommodate the different mimetics. Like glutamate, the γ-carboxyl-mimicking moieties of all modelled compounds are able to accept a hydrogen bond from the side chain of Asn257 and form a strong salt bridge with the side chain of Lys699. The second salt bridge is formed between the α-carboxylate group of all four compounds and the side chain of Arg210.

4. Discussion

Crystal structures of the extracellular part of GCPII (amino-acid residues 44–750) in complex with either quisqualate (α-amino-3,5-dioxo-1,2,4-oxadiazolidine-2-propanoic acid) or 2-PMPA (2-phosphonomethyl pentanedioic acid) were determined by difference Fourier methods. The X-ray structures and the overall binding mode of the two inhibitors in the S1′ site are comparable to those recently reported for glutamic acid and GPI-18431, respectively (Mesters *et al.*, 2006). However, quisqualate appears to require more space in the S1′ pocket owing to its 3,5-dioxo-1,2,4-oxadiazolidine moiety. In response, residues Lys699 and especially Asn257 adapt their side-chain conformation (compare Figs. 2*b* and 2*c*), demonstrating some plasticity of the S1′ pocket.

On the basis of the current X-ray structures, we constructed models for S1′-bound willardiine, homoibotenate (HIBO), L-2-amino-4-phophonobutanoic acid (L-AP4) and L-serine-*O*-sulfate (L-SOS) (Fig. 3). All these compounds can be considered to be bona fide glutamate analogues. More precisely, the side chains of all the compounds that enter the GCPII S1′ pocket share a great similarity to a γ-carboxyl group in that they feature at least two O atoms and moreover bear a negative charge. These properties enable the side chains to accept a hydrogen bond from Asn257 and, most importantly, form an ionic interaction with Lys699 of the glutarate-sensor clamp (Mesters *et al.*, 2006).

Many of the glutamate-like inhibitors discussed here display dual effects: for example, 2-PMPA not only inhibits GCPII itself but is also reported to affect a downstream target of glutamate, the group II metabotropic glutamate-receptor subtype 3 ($mGluR_3$; US Patent 6 528 499; see also Nan *et al.*, 2000). The same holds true for quisqualate. The mGluR-directed 2-methylated derivatives of L-serine-*O*-phosphate (called MSOP) and L-AP4 (called MAP4) might also inhibit GCPII. However, a compound such as L-theanine (γ-glutamylethylamide) from green tea, which was reported to bind to mGluR, will probably not bind strongly to GCPII since its side chain bears no negative charge.

With an IC_{50} value of $\sim$0.3 n*M*, 2-PMPA is the strongest inhibitor of GCPII reported to date (Jackson & Slusher, 2001; Tsukamoto *et al.*, 2005; Majer *et al.*, 2006). In comparison to glutamate (IC_{50} value of $\sim$30 μM; Robinson *et al.*, 1987), 2-PMPA possesses an additional α-phosphono moiety that strongly binds to the active-site zinc ions. However, small substances that bear three negative charges pose a non-favourable starting point for the design of lead compounds that could later be turned into drugs with excellent pharmacokinetic properties because they would violate the 'rule of five' (Lipinski *et al.*, 2001; Ghose *et al.*, 1999). In particular, they can be predicted to exhibit low oral availability because of a poor partition coefficient ($\log P < -2$; see Van de Waterbeemd, 2003). However, attaching uncharged P1 substituents to the 2-PMPA scaffold has so far reduced affinity (Jackson & Slusher, 2001). On the other hand, smaller compounds that exclusively bind to the S1′ pocket without coordinating the zinc ions lack high affinity/specificity for GCPII. Specificity is needed in order to evade the dual effects discussed above. No compounds

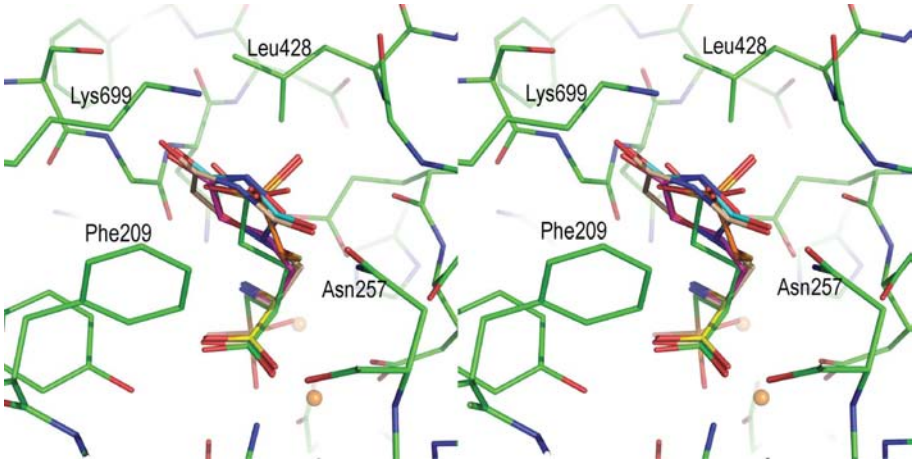

Figure 3
Stereo diagram showing the superimposition of all inhibitors in the S1′ pocket. 2-PMPA, green; L-AP4, orange; L-SOS, yellow; quisqualate, turquoise; HIBO, pink; willardiine, wheat. Zinc ions are shown as small spheres.

have been reported to date that solely bind to the large amphipathic S1 site. 3,4-Dichloroisocoumarin has been shown to inhibit GCPII (Luthi-Carter *et al.*, 1998), but we have no clear idea of where it could bind, although one could speculate that it might occupy the S1 site.

One possible route towards stronger and more specific inhibitors is to make use of both the S1 and S1′ pockets while reducing the overall net charge. Dipeptides featuring, for example, a methionine instead of a glutamate in the C-terminal P1′ position, however, cannot form an ionic interaction or hydrogen bond with Lys699 and it is therefore not surprising that the k_{cat}/K_M of GCPII for *N*-acetyl-L-aspartyl-L-methionine is ∼500-fold lower (Barinka *et al.*, 2002) than that for the natural substrate *N*-acetyl-L-aspartyl-L-glutamate. Another possibility is to try and reduce the net charge of possible lead compounds such as 2-PMPA and make full use of the structure-based observation that the S1′ pocket has a clear amphiphatic character with two opposing hydrophobic walls, Phe209 and Leu428, which are connected by Gly518, Lys699 and Asn257. Extended (partly) hydrophobic compounds that bear at least one oxygen/OH group, or even a negative charge, can be expected to bind with appreciable affinity to the S1′ pocket. The latter can be easily derived from a comparison of the structures and IC_{50} values of L-glutamate (∼30 μ*M*) and L-quisqualate (∼0.48 μM), *i.e.* quisqualate exploits the properties of the S1′ pocket far better than a glutamate as present in the natural substrates. Surely, the affinities, and probably specificities, of compounds such as quisqualate, homoibotenate or willardiine could be drastically enhanced by attaching a mercapto moiety (a zinc-ion chelator; see Suh *et al.*, 1995) analogous to that in 3-(2-carboxy-5-mercaptopentyl)benzoic acid (IC_{50} = 15 n*M*; Majer *et al.*, 2006) while gaining oral availability.

The authors thank Cyril Barinka and Jan Konvalinka for providing recombinant human GCPII and Guilford Pharmaceuticals Inc. (Baltimore, MD, USA) for inhibitors. RH thanks the Fonds der Chemischen Industrie for continuous support.

References

Barinka, C., Rinnova, M., Sacha, P., Rojas, C., Majer, P., Slusher, B. S. & Konvalinka, J. (2002). *J. Neurochem.* **80**, 477–487.
Cohen, G. E. (1997). *J. Appl. Cryst.* **30**, 1160–1161.
Collaborative Computational Project, Number 4 (1994). *Acta Cryst.* D**50**, 760–763.
Davis, M. I., Bennett, M. G., Thomas, L. M. & Bjorkman, P. J. (2005). *Proc. Natl Acad. Sci. USA*, **102**, 5981–5986.
Emsley, P. & Cowtan, K. (2004). *Acta Cryst.* D**60**, 2126–2132.
Flippen, J. L. & Gilardi, R. D. (1976). *Acta Cryst.* B**32**, 951–953.
Ghose, A. K., Viswanadhan, V. N. & Wendoloski, J. J. (1999). *J. Comb. Chem.* **1**, 55–68.
Jackson, P. F., Cole, D. C., Slusher, B. S., Stetz, S. L., Ross, L. E., Donzanti, B. A. & Trainor, D. A. (1996). *J. Med. Chem.* **39**, 619–622.
Jackson, P. F. & Slusher, B. S. (2001). *Curr. Med. Chem.* **8**, 949–957.
Koller, K. J. & Coyle, J. T. (1985). *J. Neurosci.* **5**, 2882–2888.
Lipinski, C. A., Lombardo, F., Dominy, B. W. & Feeney, P. J. (2001). *Adv. Drug. Deliv. Rev.* **46**, 3–26.
Luthi-Carter, R., Barczak, A. K., Speno, H. & Coyle, J. T. (1998). *Brain Res.* **795**, 341–348.
Majer, P., Hin, B., Stoermer, D., Adams, J., Xu, W., Duvall, B. R., Delahanty, G., Liu, Q., Stathis, M. J., Wozniak, K. M., Slusher, B. S. & Tsukamoto, T. (2006). *J. Med. Chem.* **49**, 2876–2885.
Mesters, J. R., Barinka, C., Li, W., Tsukamoto, T., Majer, P., Slusher, B. S., Konvalinka, J. & Hilgenfeld, R. (2006). *EMBO J.* **25**, 1375–1384.
Murshudov, G. N., Vagin, A. A. & Dodson, E. J. (1997). *Acta Cryst.* D**53**, 240–255.
Nan, F., Bzdega, T., Pshenichkin, S., Wroblewski, J. T., Wroblewska, B., Neale, J. H. & Kozikowski, A. P. (2000). *J. Med. Chem.* **43**, 772–774.
Rawlings, N. D., Tolle, D. P. & Barrett, A. J. (2004). *Nucleic Acids Res.* **32**, D160–D164.
Robinson, M. B., Blakely, R. D., Couto, R. & Coyle, J. T. (1987). *J. Biol. Chem.* **262**, 14498–14506.
Schulke, N., Varlamova, O. A., Donovan, G. P., Ma, D., Gardner, J. P., Morrissey, D. M., Arrigale, R. R., Zhan, C., Chodera, A. J., Surowitz, K. G., Maddon, P. J., Heston, W. D. & Olson, W. C. (2003). *Proc. Natl Acad. Sci. USA*, **100**, 12590–12595.
Slusher, B. S., Vornov, J. J., Thomas, A. G., Hurn, P. D., Harukuni, I., Bhardwaj, A., Traystman, R. J., Robinson, M. B., Britton, P., Lu, X. C., Tortella, F. C., Wozniak, K. M., Yudkoff, M., Potter, B. M. & Jackson, P. F. (1999). *Nature Med.* **5**, 1396–1402.
Speno, H. S., Luthi-Carter, R., Macias, W. L., Valentine, S. L., Joshi, A. R. & Coyle, J. T. (1999). *Mol. Pharmacol.* **55**, 179–185.
Stauch, B. L., Robinson, M. B., Forloni, G., Tsai, G. & Coyle, J. T. (1989). *Neurosci. Lett.* **100**, 295–300.
Suh, J., Lee, S. H. & Uh, J. Y. (1995). *Bioorg. Med. Chem. Lett.* **5**, 585–588.
Troyer, J. K., Beckett, M. L. & Wright, G. L. Jr (1995). *Int. J. Cancer*, **62**, 552–558.
Tsukamoto, T., Majer, P., Vitharana, D., Ni, C., Hin, B., Lu, X. C. M., Thomas, A. G., Wozniak, K. M., Calvin, D. C., Wu, Y., Slusher, B. S., Scarpetti, D. & Bonneville, G. W. (2005). *J. Med. Chem.* **48**, 2319–2324.
Van de Waterbeemd, H. (2003). *Modern Methods of Drug Discovery*, edited by A. Hillisch & R. Hilgenfeld, pp. 243–257. Basel: Birkhäuser Verlag.